



Article

# Early Diagnosis of Alzheimer's Disease Using Cerebral Catheter Angiogram Neuroimaging: A Novel Model Based on Deep Learning Approaches

Maha Gharaibeh <sup>1</sup>, Mothanna Almahmoud <sup>2,\*</sup>, Mostafa Z. Ali <sup>2</sup>, Amer Al-Badarneh <sup>2</sup>, Mwaffaq El-Heis <sup>1</sup>, Laith Abualigah <sup>3,4</sup>, Maryam Altalhi <sup>5</sup>, Ahmad Alaiad <sup>2</sup> and Amir H. Gandomi <sup>6,\*</sup>

<sup>1</sup> Department of Diagnostic Radiology and Nuclear Medicine, Jordan University of Science and Technology, Irbid 22110, Jordan; mmgharaibeh@just.edu.jo (M.G.); maelheis@just.edu.jo (M.E.-H.)

<sup>2</sup> Department of Computer Information Systems, Jordan University of Science and Technology, Irbid 22110, Jordan; mzali@just.edu.jo (M.Z.A.); amerb@just.edu.jo (A.A.-B.); aiaiad@just.edu.jo (A.A.)

<sup>3</sup> Faculty of Computer Sciences and Informatics, Amman Arab University, Amman 11953, Jordan; aligah.2020@gmail.com

<sup>4</sup> School of Computer Sciences, Universiti Sains Malaysia, Gelugor 11800, Malaysia

<sup>5</sup> Department of Management Information System, College of Business Administration, Taif University, P.O. Box 11099, Taif 21944, Saudi Arabia; marem.m@tu.edu.sa

<sup>6</sup> Faculty of Engineering and Information Technology, University of Technology Sydney, Ultimo, NSW 2007, Australia

\* Correspondence: mr.mothanna@gmail.com (M.A.); Gandomi@uts.edu.au (A.H.G.)



**Citation:** Gharaibeh, M.; Almahmoud, M.; Ali, M.Z.; Al-Badarneh, A.; El-Heis, M.; Abualigah, L.; Altalhi, M.; Alaiad, A.; Gandomi, A.H. Early Diagnosis of Alzheimer's Disease Using Cerebral Catheter Angiogram Neuroimaging: A Novel Model Based on Deep Learning Approaches. *Big Data Cogn. Comput.* **2022**, *6*, 2. <https://doi.org/10.3390/bdcc6010002>

Academic Editors: Moulay A. Akhloufi and Mustapha Kardouchi

Received: 29 November 2021

Accepted: 21 December 2021

Published: 28 December 2021

**Publisher's Note:** MDPI stays neutral with regard to jurisdictional claims in published maps and institutional affiliations.



**Copyright:** © 2021 by the authors. Licensee MDPI, Basel, Switzerland. This article is an open access article distributed under the terms and conditions of the Creative Commons Attribution (CC BY) license (<https://creativecommons.org/licenses/by/4.0/>).

**Abstract:** Neuroimaging refers to the techniques that provide efficient information about the neural structure of the human brain, which is utilized for diagnosis, treatment, and scientific research. The problem of classifying neuroimages is one of the most important steps that are needed by medical staff to diagnose their patients early by investigating the indicators of different neuroimaging types. Early diagnosis of Alzheimer's disease is of great importance in preventing the deterioration of the patient's situation. In this research, a novel approach was devised based on a digital subtracted angiogram scan that provides sufficient features of a new biomarker cerebral blood flow. The used dataset was acquired from the database of K.A.U.H hospital and contains digital subtracted angiograms of participants who were diagnosed with Alzheimer's disease, besides samples of normal controls. Since each scan included multiple frames for the left and right ICA's, pre-processing steps were applied to make the dataset prepared for the next stages of feature extraction and classification. The multiple frames of scans transformed from real space into DCT space and averaged to remove noises. Then, the averaged image was transformed back to the real space, and both sides filtered with Meijering and concatenated in a single image. The proposed model extracts the features using different pre-trained models: InceptionV3 and DenseNet201. Then, the PCA method was utilized to select the features with 0.99 explained variance ratio, where the combination of selected features from both pre-trained models is fed into machine learning classifiers. Overall, the obtained experimental results are at least as good as other state-of-the-art approaches in the literature and more efficient according to the recent medical standards with a 99.14% level of accuracy, considering the difference in dataset samples and the used cerebral blood flow biomarker.

**Keywords:** deep learning; diagnosis; Alzheimer's disease; neuroimaging

## 1. Introduction

Neuroimaging refers to a group of imaging techniques that aim to visualize the nervous system; it is one of the most powerful disciplines within neuroscience [1]. The rapid development of these techniques resulted in new images, which assisted the extraction of critical details for brain structure and functionality [2]. Besides, these images are utilized by medical staff, radiologists, and researchers for important purposes, namely, treatment

process, early diagnostic, and conducting new scientific research. Recently, neuroimaging modalities, such as Magnetic Resonance Imaging (MRI), Computed Tomography (CT), and Positron Emission Tomography (PET) became an effective source for researchers, which they use to devise new systems for neuroimages processing [3]. The processing of neuroimages has an important role in diagnostic classification, where it helps to extract hidden features based on image pixels. The accurate results of processing assist in differentiating between the normal and infected cases, which reveal through detecting the unusual characteristics of the image [4]. From this standpoint, it can be stated that neuroimages processing is the main assistant for medical staff and expert radiologists to make an optimal diagnosis of accurate results, without wasting more and more time on the classical methods.

Diagnostic classification methods differ based on the used procedure. The most common method is the classical classification, where the expert radiologists extract the features of neuroimage, manually. This method requires a long time, and experts who are trained, perfectly. Additionally, the chance of error is high due to the different opinions of trained experts. Conversely, the automated systems are more accurate and save time, where it includes automatic methods for neuroimage processing [5]. These methods are built based on machine learning algorithms, which performs feature extraction, early detection, and classification based on training and testing datasets that include normal and infected cases. Nowadays, machine learning algorithms are used widely for neuroimages classification in several tasks, like neurology [6]. Nonetheless, each of these methods has different characteristics in terms of time-consuming and accuracy, which has been led to valuable competition between the researchers to devise more and more methods with optimal results.

The new approaches of deep learning, especially the Convolutional Neural Network (CNN) [7], achieved valuable success in different tasks of computer vision, such as object detection, segmentation, and classification. The techniques of CNN are distinguished by the high level of efficiency in image processing, as it can be utilized for performing both feature extraction and classification, while classical machine learning techniques still lean on distinct techniques to extract features and feed them into classifiers. Feature extraction of an image refers to applying a convolutional filter that generates a feature map followed by a pooling layer that helps to reduce the map size. Transfer learning refers to reuse of developed model, where the model is trained on a wide range of data. In transfer learning, the network model uses a pre-trained network with preset weights. The success of using pre-trained models has attracted researchers recently to conduct many studies in the field of medical images.

The aim of this work is to devise an effective model for the early diagnosis of Alzheimer's disease based on the Digital Subtracted Angiogram (DSA) neuroimages. Arterial and vascular diseases are considered as contributing factors to Alzheimer's disease [8]. Besides, there is a relationship between the reduction of cerebral blood flow and Alzheimer's disease [9]. The patients with Alzheimer's disease experience a decrease of approximately 0.30 percent in blood flow to the brain [10], and that is caused by cerebral vascular dysfunction, which can be described as diminished blood vessel diameter and loss of small blood vessels [11,12], the background section provided further details. Alzheimer's disease is a brain irreversible disorder, where patients experience a gradual decline in cognitive performance over time [13]. Additionally, the early diagnosis of Alzheimer's disease is considered as one of the most difficult tasks, because of the various causes and symptoms [14]. Usually, it is diagnosed by expert radiologists and neurologists through using MRI and PET images. However, this classical method of diagnosis is difficult, time-consuming, and has a poor rate of error.

To reach our aim, we have collected a dataset of DSA scans from the database of King Abdullah University Hospital according to the institutional review boards approval. contains DSA scans for 13 patients of Alzheimer's disease and other 27 normal controls, which were selected to utilize for model training and testing. The goal is to early detect the existence of Alzheimer's disease in the brain accurately. This research proposes a

novel model for the diagnosis of Alzheimer's disease by utilizing deep learning techniques along with classical machine learning algorithms. The proposed model consists of different pre-trained models, namely InceptionV3, and DenseNet201, and different classical machine learning algorithms, namely, Support Vector Machine (SVM), Logistic Regression (LR), Linear Discriminative Analysis (LDA), and Stochastic Gradient Decent (SGD). First, the number of frames for both ICA sides is reduced into one frame, where each channel is decomposed into local patches, then denoised by thresholding in the Discrete cosine transform (DCT) domain and averaged to generate the final image. Then, the Meijering neuriteness filter was performed to show the ridges of the vessels in the frames. Consequently, the filtered frames are combined in a single image. After applying data augmentation, both pre-trained models were utilized to extract features, and a combination of features selected from applying the Principal Component Analysis (PCA) technique for feature selection were fed into classifiers to obtain a high level of accuracy for Alzheimer's disease detection. The main contributions of this work concluded as the utilization of a new biomarker by using a new neuroimaging tool for the first time, and the utilization of different pre-trained deep learning models for feature extraction, besides integrating it to classical machine learning algorithms.

The rest of this research is organized as follows: Section 2 provides detailed background information about Alzheimer's disease, neuroimaging, and deep learning techniques that have been used in this field. Additionally, the section puts the spotlight on the latest previous works of early diagnosis of Alzheimer's disease and the used deep learning approaches. Section 3 presents a description of the dataset and the proposed methodology of building the early diagnostic model, including the pre-processing workflow, neural network architecture, training procedure, and evaluation strategy. Section 4 presents the experiments and results, besides a comparison between the previous works and the proposed work. Finally, Section 5 concludes the research and discusses the potential directions for future work.

## 2. Background and Literature Review

### 2.1. Background

The neural system controls all senses, decision-making, and every minor or major reflex of the human body, where any effect on this system might result in disease. Dementia is one of the neural system diseases that is caused by damage or loss of nerve cells and their connections to the brain [15], where it affects people differently and causes different symptoms. According to the National Institute of Neurological Disorders and Stroke [16], Alzheimer's disease is the most common form of dementia that attacks brain cells and neurotransmitters, affecting the way humans' brain functions, their memory, and the way they behave. At the beginning of the 21st century, it was thought that most people with dementia had Alzheimer's disease [17].

Alzheimer's disease is an irreversible brain disorder in which patients experience a gradual decline in cognitive performance [13]. The lifetime risk of Alzheimer's disease in people aged 65 years was estimated to be 10.5% [18]. In a study that revealed the overall burden of Alzheimer's disease through systematic analysis [19], the researchers have found that the number of infected people increases dramatically over time with the number more than doubling during the period from 1990 to 2016. The efforts of researchers continue to find an effective treatment for this disease, which in turn has placed a heavy burden on healthcare providers around the world. Moreover, it has a negative impact on patients in many aspects, such as social behaviors, with an impact on careers, family, and society at large that can be physical, psychological, social, and economic.

The National Institute on Aging and the Alzheimer's Association of the United States have published guidelines that postulate three stages of Alzheimer's disease [20]. The first stage is the preclinical phase, which shows the existence of unusual biomarker patterns, such as the low rate of amyloid- $\beta$  in cerebrospinal fluid or the high rate of amyloid tracer retention. The second stage is mild cognitive impairment, which can be diagnosed using

additional biomarkers and imaging technology. The third stage is Alzheimer's dementia, which requires further study to provide efficient biomarkers.

Biomarkers of Alzheimer's disease include tau-related proteins, amyloid- $\beta$ , cerebral hypometabolism, brain atrophy, and cognitive functioning [21]. The availability of these biomarkers and the interrelationship between them have made it difficult to find the importance of each one, independently. Since it is difficult to establish both putative and additive weights for biomarkers of Alzheimer's disease, recent researches tend to use a combination of biomarkers from different modalities to enhance the performance of models for Alzheimer's disease detection.

Until 2018, the global cost of managing Alzheimer's disease has increased, and this has negatively affected the overall economy [22]. The efforts to develop tools that can identify indicators associated with Alzheimer's disease have emerged as advanced neuroimaging techniques, such as Computerized Tomography, Magnetic Resonance Imaging, Magnetic Resonance Angiogram, and Positron Emission Tomography [23]. Table 1 shows the uses, advantages, and disadvantages of neuroimaging techniques.

**Table 1.** The uses, advantages, and disadvantages of neuroimaging techniques.

Neuroimaging	Uses	Advantages	Disadvantages
CT	Determine brain atrophy	Short time study and high quality	Requires large radiation doses
SPECT	Determine Beta-amyloid deposition and neurofibrillary tangles	Well-supplied and has a low cost	Not able to differentiate between Alzheimer's and other Dementia diseases
MRI	Analyze vital signs of neuronal loss	Distinguish between Alzheimer's disease and other Dementia diseases	Very expensive and time-consuming
MRA	Evaluate age-related changes in the cerebral arteries	Detect dementia diseases	Difficult to evaluate small vessels
PET	Reveal tissues and organs functions	Evaluate brain amyloid	Erroneous interpretations

Computerized Tomography (CT) is the first human brain neuroimaging tool, as well as the first choice for diagnosing Alzheimer's disease [24]. Specific brain atrophy is one of the most important indicators that are associated with cerebral vascular disease; where studies and experiments have shown that determining this indicator through CT scans contribute efficiently to accurate diagnosis of Alzheimer's disease [25]. In general, a CT scan has the advantage of short study time with high-quality images, but patients are required to be exposed to radiation and use a contrast material to have a CT scan, which is inappropriate for those who suffer from kidney problems [26].

Single-Photon Emission Computerized Tomography (SPECT), which is a cerebral blood flow imaging technique, is one of the types of brain neuroimaging used to detect Alzheimer's disease, where it can use to determine Beta-amyloid deposition and neurofibrillary tangles [27]. In addition, it is well supplied and has a low cost compared to other types of neuroimaging types. Although it is not able to differentiate between Alzheimer's and other dementia diseases, it is good to use in conjunction with other neuroimaging types [28].

Magnetic Resonance Imaging (MRI) is a type of brain imaging that is used for the purposes of clinical evaluation of Alzheimer's patients, by analyzing the vital signs of neuronal loss [29]. It is not only used to detect Alzheimer's disease, but this type of image is good enough to be used to distinguish between Alzheimer's disease and other dementia diseases [30]. However, MRI is a very expensive and time-consuming investigation compared to other neuroimaging techniques [31].

Magnetic Resonance Angiography (MRA) is one of the most common causes of dementia is cerebral vascular degeneration, which refers to the terminal diseases that affect the

cerebral arteries [32,33]. MRA is one of the best methods for detecting dementia diseases, as it is used to evaluate age-related changes in the cerebral arteries [34]. However, it is difficult to evaluate small vessels using MRA, and it may not be as clear as catheter angiography scans [35].

Positron Emission Tomography (PET) and Fluorodeoxyglucose-PET (FDG-PET) scans are imaging techniques that reveal how tissues and organs are functioning in human body [36], where both scans are used to evaluate brain amyloid and are useful in excluding significant amyloid deposition. However, PET and FDG-PET have limitations, where the movements of the patient's head during scanning generate artifacts that may lead to erroneous interpretation of the study. Table 2 shows the most common neuroimaging databases that can be utilized for Alzheimer's disease detection, including the types of neuroimaging it contains.

**Table 2.** Neuroimaging databases for Alzheimer's disease.

Database	PET	SPECT	MRI	CT
ADNI [37]	Yes	No	Yes	No
HMSD [38]	Yes	Yes	Yes	Yes
OASIS [39]	No	No	Yes	No

Alzheimer's Disease Neuroimaging Initiative (ADNI) is an association of universities and medical centers, which are the basis in Canada and USA [37], have developed the ADNI dataset to provide researchers with open-source datasets. ADNI datasets include different types of neuroimaging that are utilized to discover features related to Alzheimer's disease diagnosis. The participants are patients diagnosed with Alzheimer's disease and mild cognitive impairment, besides normal control, and elderly control cases. Neuroimaging types include MRI and PET scans, in addition to some biochemical and clinical data. Specifically, there are four phases of ADNI datasets, which are, ADNI-1, ADNI-GO, ADNI-2, and ADNI-3.

Harvard Medical School Dataset (HMSD) dataset conducted by Harvard medical school [38], where consists of MRI, CT, SPECT, and PET scans for 613 patients diagnosed with different types of dementia including Alzheimer's disease. An open-access dataset can be utilized by researchers to extract features from different modalities that assist the development of early diagnosis methods.

Open Access Series of Imaging Studies (OASIS) datasets conducted by Howard Hughes Medical Institute at Harvard University [39], in association with the Neuroinformatics Research Group at Washington University School of Medicine and the Biomedical Informatics Research Network. The dataset consists of MRI neuroimaging data for 18–96 year old participants who have been diagnosed by Alzheimer's disease.

In a medical study on finding a relationship between Alzheimer's disease and the aging of cerebral blood vessels [8], the researchers have conducted an evaluation review of the changes in the blood vessels of Alzheimer's patients, and the results indicated that vascular disease is one of the contributing factors to Alzheimer's disease. Based on the results, it can be concluded that arterial and vascular diseases could be two good measures that should be considered to take preventive actions and therapeutic treatment for Alzheimer's disease, where the researchers have recommended the need to conduct more researches from this perspective to find a cure. Furthermore, the results of other research [40–42] have proved that there is evidence of increased cerebral blood flow in the early stages of Alzheimer's disease, which is followed by a reduction phase of cerebral blood flow.

Choosing the biomarker is important to start looking for treatment for the disease, and this is what the researchers pointed out for Alzheimer's disease in [43,44], where they recommended the use of techniques that focus on the harmful reduction of cerebral blood flow. Besides, there is a relationship between low cerebral blood flow and Alzheimer's disease [9].

Furthermore, patients with Alzheimer's disease have been shown to have approximately a 30% reduction in blood flow to the brain [45]. Moreover, cerebral vascular dysfunction is a major cause of reduced cerebral blood flow, as it is described as a diminished blood vessel diameter and loss of small blood vessels [46,47]. Examples of carotid artery diseases are stenosis and occlusion. Stenosis refers to the narrowing of carotid arteries caused by the buildup of fatty substances and cholesterol deposits, called plaque. Even more, occlusion refers to a worsening condition of stenosis with a clot, which is defined as a complete blockage of the artery. These diseases are the most common contributing factors that cause a reduction of cerebral blood flow.

The previous studies have not addressed the use of all types of neuroimaging for the diagnosis of Alzheimer's disease. Some of the most unused neuroimaging data are from DSA scans, which are a catheter cerebral angiography used to reveal accurate anatomical information for cerebral blood vessels and are considered a good indicator to diagnose and monitor Alzheimer's disease conditions [48]. DSA is the golden standard to diagnose and build a treatment plan for patients who are suffering from vascular anomaly, because of its high-resolution anatomical data about the cerebral blood vessels, besides the ability to analyze the blood flow in real-time [49]. Therefore, it is possible to use DSA data in the early detection and diagnosis of Alzheimer's disease because it carries strong indicators that are characterized by very high accuracy, sensitivity, and specificity.

## 2.2. Literature Review

Recently, the emergence of technological development has led to the introduction of modern technologies that are helpful to healthcare providers, including the development in the neuroimaging process, which has assisted medical staff and researchers in obtaining a huge amount of different neuroimaging data sets.

### 2.2.1. Classical Machine Learning-Based Methods

As part of the developments, machine learning algorithms have also been introduced, which has had a great impact in speeding up the process of detecting and treating Alzheimer's disease. Machine learning has helped build predictive models for early detection of Alzheimer's disease, where researchers have used known pattern analysis methods, such as linear discrimination analysis (LDA), logistic regression (LR), and support vector machine (SVM) [50]. In fact, the use of these traditional classification methods requires expertise and multiple stages of improvement, and thus, the biggest barrier to using them is a long time required to complete these stages [51].

Lebedev et al. [52] conducted a study to build a diagnosis model for Alzheimer's disease. They used structural MRI images of 185 Alzheimer's patients and 225 normal subjects from the ADNI database. They have used the Free-Surfer image analysis software that incorporates the surface-based registration approach to extract the average morphometric features, which are sulcal depth, Jacobian maps, and cortical thickness. During the training process, they have used out of bag estimation to tune and assess the model performance, and RF has obtained the highest performance with 88.6% and 92.0% of sensitivity and specificity, respectively.

Zhang and Wang [53] used 3D-MRI scans for 28 patients with Alzheimer's disease and 98 normal subjects from the OASIS database, where the displacement field fed as the features after reducing it using principal component analysis technique for dimensionality reduction. Based on the results, the Twin-SVM classifier has obtained the highest performance with 92.75%, 90.56%, and 79.61% of accuracy, sensitivity, and specificity, respectively.

Furthermore, Beheshti et al. [54] used structural MRI scans for 130 Alzheimer's patients and 130 normal subjects from the ADNI database, where each participant has performed neuropsychological exams, in which they obtained clinical indicators, which are the scores of mini-mental state examination and clinical dementia ratio. Besides, they used the voxel-based feature extraction technique to extract features from structural MRI scans and the

feature ranking obtained through minimizing the error of classification. Based on the results, their proposed model has obtained a high performance with 92.48% accuracy.

In another study, Zhang et al. [55] used the longitudinal structural MRI scans for 154 Alzheimer's patients and 207 normal subjects from the ADNI database. Then, they utilized a data-driven landmark discovery algorithm to obtain landmarks and proposed a landmark-based framework for feature extraction that uses a bag-of-words strategy to extract statistical high-level spatial and contextual longitudinal features. Based on their results, the SVM classifier obtained a high performance with an 88.30% rate of accuracy.

Zeng et al. [56] used MRI scans for 92 Alzheimer's patients and 82 patients with NC from the ADNI database. Then, they utilized the automated anatomical labeling template to extract voxel features. They proposed a hybrid model that optimizes the kernel parameter and penalty factor of the SVM classifier using the switching delayed particle swarm optimization algorithm and principal component analysis. Based on the result, the proposed classifier has outperformed other machine learning classifiers with a 71.23% level of accuracy.

Lately, Koh et al. [57] used MRI brain scans for 55 Alzheimer's patients and 110 normal subjects from Harvard Brain Atlas and the University of Malaya Medical Centre databases. Then, they utilized the bidirectional empirical mode decomposition technique to extract features. Based on the results, SVM with polynomial kernel of one degree and RF classifiers have obtained the highest performance with a 93.9% level of accuracy.

Accordingly, the use of traditional machine learning requires a mandatory stage to extract features from different neuroimaging scans and feed them to classification algorithms, which is the biggest barrier as it takes a long time.

### 2.2.2. Deep Learning-Based Methods

Deep learning could overcome the difficulties encountered by researchers while using traditional approaches of machine learning in dealing with images. It was met with great interest in the field of image processing, primarily in medicine [58]. The results of using deep learning algorithms demonstrated a clear superiority over the performance of traditional machine learning techniques [59], which is why they are highlighted as the best methods for dealing with images datasets.

Liu et al. [60] conducted a study to build a model to diagnose Alzheimer's disease using deep learning approaches based on FDG-PET neuroimaging. They used 3D-FDG-PET scans for 93 patients with Alzheimer's disease and 100 normal subjects from the ADNI database, and they divide it into 2D slices. Then, slices were grouped based on the structure similarity, where each group included nine slices. Deep learning approaches were utilized for feature extraction, in which they trained a 2D-CNN model to extract the intra-slice features and 2-stacked bidirectional-gated recurrent unit cascaded to capture the interslice features. The final classification output is generated based on feeding the generated features into two fully connected layers and a softmax layer. Based on the result, the proposed model has a high performance with a 91.2% level of accuracy.

Ge et al. [61] used 3D MRI scans for 198 patients with Alzheimer's disease and 139 normal subjects from the ADNI database. A 3D-multiscale-CNN was constructed to extract the multiresolution features, and parallel 3D multiscale-CNNs were performed on three regions of the tissue image, which are cerebrospinal fluid, white matter, and grey matter. Besides, two separate levels of fusion layer were performed on several scales of a tissue region and different tissue regions. Then, XGBoost [62] was used for dimensionality reduction of the produced features, besides the classification task. Based on the results, the proposed model has achieved an 89.51% level of accuracy on datasets separated by subject.

Basaia et al. [63] used MRI scans for 124 patients with Alzheimer's disease and 50 normal subjects from the Milan database, besides 418 patients with Alzheimer's disease and 407 normal subjects from the ADNI database. The proposed model includes 12 convolutional layers repeated blocks with ReLU activation function followed by a fully connected layer

and LR output layer. Based on the results, the proposed model has obtained high performance on both data sets, in which it has achieved a 98% level of accuracy.

Furthermore, Pan et al. [64] used three-axis slices of MRI scans for 137 patients with Alzheimer's disease and 162 normal subjects from the ADNI database. The proposed model utilized the number of 2D-CNN models for feature extraction from a set of MRI slices, which are coronal, sagittal, and transverse. Then, 2D-CNN models are integrated into a unique ensemble model that generates the output of the classification. Based on the results of applying 10-fold cross-validation on the data set, the proposed model has obtained high performance with an  $84\% \pm 5\%$  level of accuracy.

Moreover, Feng et al. [65] used 3D MRI scans for 153 patients with Alzheimer's disease and 159 normal subjects from the ADNI database. They proposed three different models, which are 2D-CNN, 3D-CNN, and 3D-CNN-SVM where 3D-CNN extracted features from scans and SVM are utilized for the classification task based on the extracted features. Based on their experimental results, the 3D-CNN-SVM model has obtained the highest performance with 99.10%, 99.40%, and 98.80% rates of accuracy, specificity, and sensitivity, respectively.

In another study, Li et al. [66] used 4D MRI scans for 116 patients with Alzheimer's disease and 174 normal subjects from the ADNI database. The proposed model was constructed using two approaches, which are 3D-CNN and Long-Short Term Memory (LSTM), in which 3D-CNN was utilized to extract features from scans using 3D convolutional kernels, while LSTM was utilized for the classification task based on the extracted features. The proposed C3d-LSTM model had trained on 4D functional MRI scans without the need of slicing it into 3D and 2D images, where 3D CNN could capture spatial features, and LSTM could capture the time-varying features. Based on their experiments, the model has obtained high performance with  $97.37\% \pm 0.56\%$  level of accuracy.

Lately, Liu et al. [67] used MRI scans for 30 patients with Alzheimer's disease and 332 normal subjects from the OASIS database, and they applied resampling techniques on the data set, where the final form contained scans for 450 patients with Alzheimer's disease and 532 normal subjects. Besides, a number of MRI scans from the ADNI database were utilized for testing their model. The proposed model is depth-wise separable CNN differs from the basic CNN, where it separates the convolutional layer into filtering and feature extracting layers. In addition, they utilized the basic CNN model besides GoogLeNet and AlexNet [68,69] through transfer learning. Based on their experiments, transfer learning has obtained the highest performance, where GoogLeNet has achieved 93.02% level of accuracy.

The results of previous studies have proved that the use of deep learning approaches is more accurate and effective than traditional machine learning techniques, in which that deep learning approach does not require a feature extraction stage. Moreover, accurate and effective results are achieved because of the image abundance used in Alzheimer's neuroimaging types. Nevertheless, deep learning approaches still need to be further improved in handling neuroimaging data, especially the datasets that contain multiple frames for each patient, where each frame contains specific features; at the end, all are connected to and indicate critical changes.

Furthermore, it appears that previous studies did not address the use of DSA scans, and no research leans on the cerebral blood flow biomarker for the purpose of diagnostic classification of Alzheimer's disease. This research is considered the first one that leans on cerebral blood flow, which is a novel biomarker examined using DSA scans. Besides, we devise a novel diagnostic approach, where the results are verified in cooperation with experts in the field of interventional radiology, through testing results accuracy as needed to obtain a competitive stand and explaining conclusions regarding impaired blood flow and its effect on Alzheimer's patients.

### 3. Methodology

This section provides a description of the proposed methodology for the early diagnosis of Alzheimer's disease. Different pre-trained CNN models were used for feature

extraction, where the primary idea aims to use a combination of features extracted using different models and fed it into machine learning algorithms for the classification task. Moreover, this section describes the use of the dataset, besides more details about the preprocessing pipeline. Figure 1 shows the workflow of the proposed methodology.

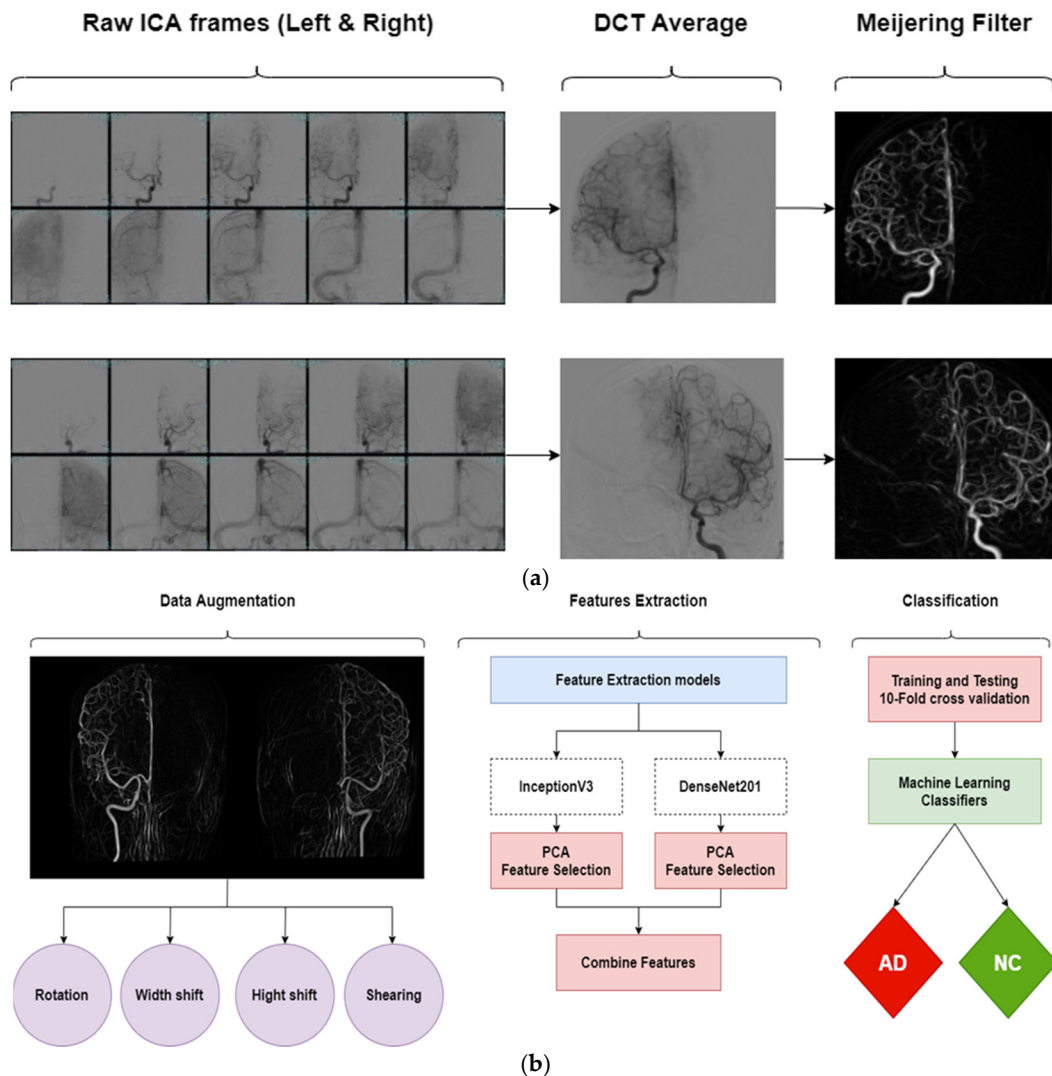


**Figure 1.** The workflow of the proposed methodology: (a) preprocessing steps after data acquisition, (b) data augmentation, features extraction, and classification.

### 3.1. Dataset Used

In this work, the dataset was acquired from the database of King Abdullah University Hospital (KAUH) according to the institutional review boards (IRBs) approval. It contains DSA scans for patients of Alzheimer's disease and other normal controls, which were selected to utilize for model training and testing. The goal is to early detect the existence of Alzheimer's disease in the brain accurately.

The procedure of DSA includes two types of imaging, namely, non-contrast images and contrast images [70]. The non-contrast imaging was used to show region anatomy and radiopaque foreign bodies, where two non-contrast images should be taken: the first one before injecting the body with the contrast material and the second one after injection. The contrast imaging was used to show the obscure vessels that were superimposed on anatomy, where these images should be taken in successive sequence during injecting the contrast material. Finally, the non-contrast image pixels are subtracted from the contrast

images pixels, and the output image of subtraction shows only vessels that were filled with blood.

The continuous recording on the computer provides multiple frames, and the data set of this work was acquired for subjects who already had the scan before. Each subject of the dataset has 10 frames—one frame per second—for both right and left internal carotid artery (ICA), which nourishes the brain's section that is responsible for memory [71]. The size of each frame is  $1024 \times 1024$  and has a single-channel grayscale. These frames show blood flow, and Figure 2 presents two samples of frames for left and right ICA.

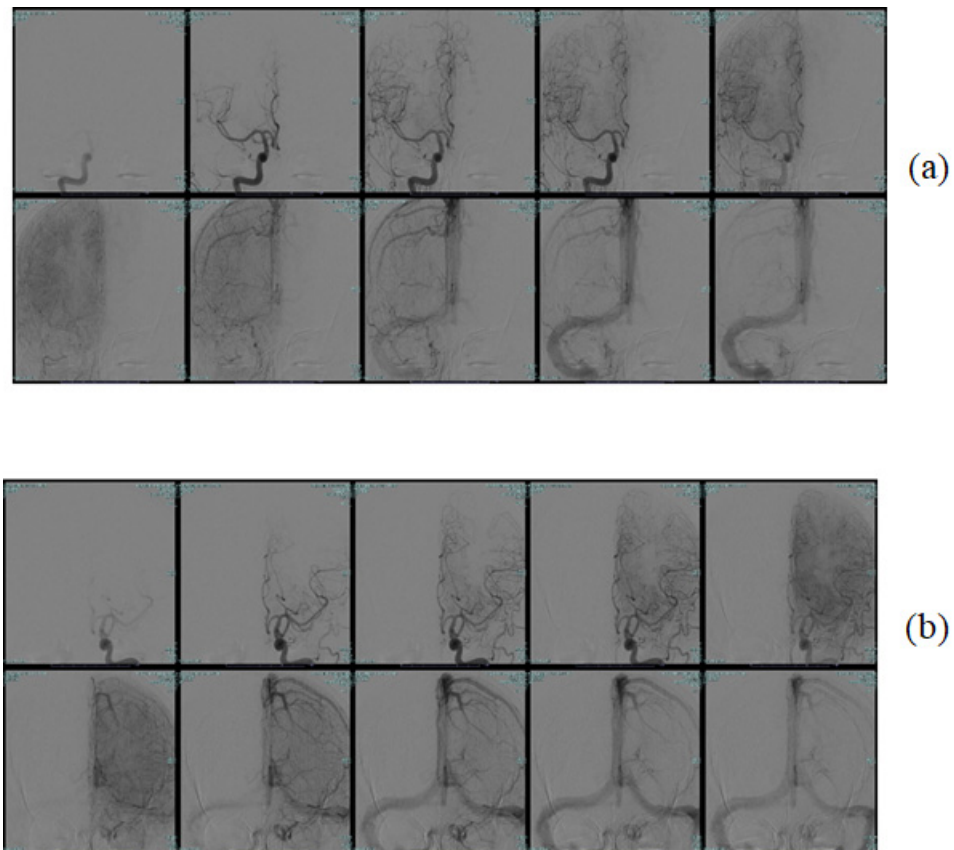


**Figure 2.** Sample of DSA scans: (a) selective right internal carotid artery, and (b) selective left internal carotid artery.

The data set includes 26 scans for patients with Alzheimer's disease and 27 scans for normal subjects. As shown in Table 3, the average age of the Alzheimer's disease group is 70 years (range from 59 to 81 years), and the average age of the normal controls group is 48 years (range from 8 years to 66 years).

**Table 3.** Summary of participants in the dataset.

Diagnostic Type	Scans No.	Age [Range]	Gender (M/F)
Normal Controls	27	$47.9 \pm 14.8$ [8–66]	15/12
Alzheimer's disease	26	$56.8 \pm 7.3$ [42–81]	14/12

Nonetheless, the vessels in the scans are not shown clearly; besides, patients' information are included in each frame. Thus, the segmentation of the vessels and masking the patient information are important steps to clean the data set. Furthermore, the acquired data set includes scans for a few participants that is why data augmentation is important

to increase the size of training and testing sets. The preprocessing methods and data augmentation of the data set can be checked in the next subsection.

### 3.2. Preprocessing and Augmentation

Essentially, data preprocessing techniques were performed to improve the quality of the dataset. First, the number of frames for both ICA sides is reduced into one frame, where each channel is decomposed into local patches. Then, it is denoised by thresholding in the discrete cosine transform (DCT) domain [72] and averaged to generate the final image. By calculating the average of frames. The images transformed from real space into DCT space based on Equation (1).

$$C(m, n) = \alpha(m)\alpha(n) \sum \sum p(x, y) \cos \left[ \frac{\pi(2x + 1)m}{2x} \right] \times \cos \left[ \frac{\pi(2y + 1)n}{2y} \right] \quad (1)$$

where  $C(m, n)$  represents the DCT's coefficients,  $p(x, y)$  represents that the image data will be performed by DCT,  $r$  is the width or length of  $p(x, y)$ ,  $m, n = 0, 1, 2, \dots, r - 1$ , and  $\alpha(m)$  is defined as in Equation (2).

$$\alpha(m) = \begin{cases} \sqrt{1/r}, & m = 0 \\ \sqrt{2/r}, & m \neq 0 \end{cases} \quad (2)$$

After the transformation in Equations (1) and (2), the resulted images in DCT space averaged to reduce the noise and transformed back into real space. Then, a bit-wise operator was utilized to mask that patients' information. Moreover, the Meijering neuriteness that refers to ridge filter [73] was performed to show the ridges of the vessels in the frames. Based on the noise level, the Meijering filter was the most appropriate to show the ridge-like structures, clearly. According to Figure 3, it can be revealed that the filter generated accurate image for two important factors that cause the problem of reduction in cerebral blood flow.

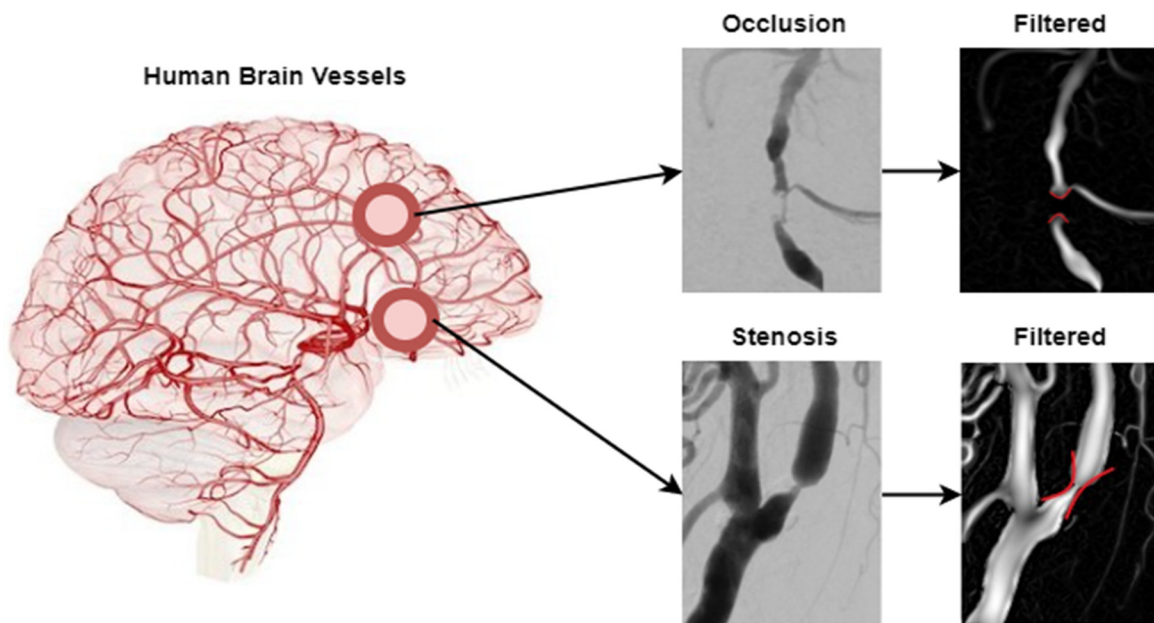


**Figure 3.** Example of how Meijering filter shows a clear DSA image of occlusion and stenosis in internal carotid arteries.

Finally, the filtered left and right ICA images are stacked in a single image, where each image represents the average of frames in DCT space after transforming back to the real space. These preprocessing steps help to prepare the dataset for the next two stages of feature extraction and classification, in which we improve the standardization

among DSA scans for different participants. Figure 4 shows the scan after performing the above-preprocessing steps.

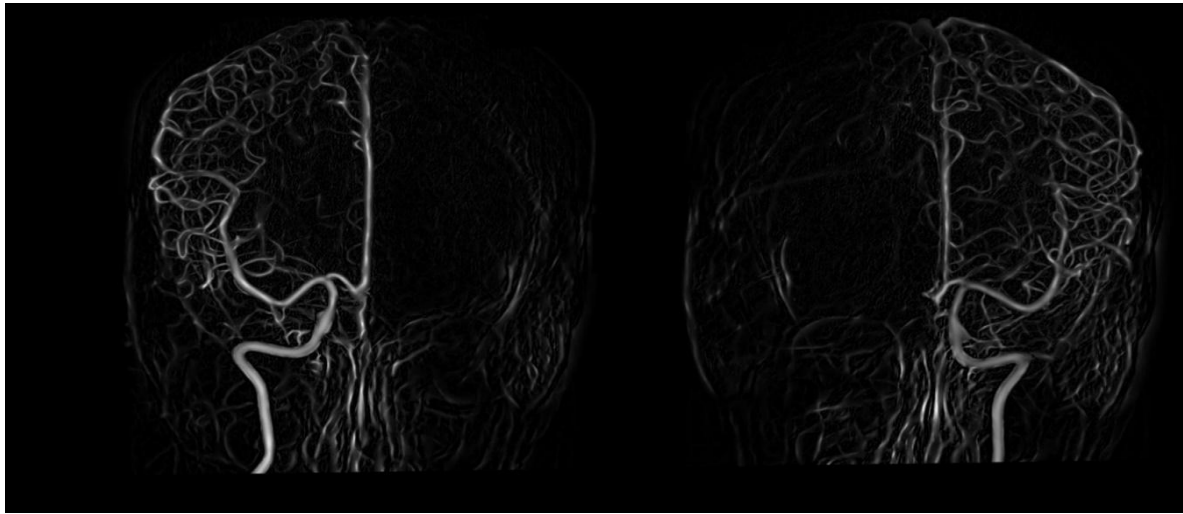


**Figure 4.** Sample of DSA scans after performing preprocessing.

Data augmentation was performed to increase the amount of data [74], in which slightly modified copies of scans were added based on the existed scans. Four samples were obtained using rotation: width shifting, height shifting, and shearing methods, where the used filling mode is constant. Thus, added samples help reduce overfitting during the training process of the model. Finally, the samples of Alzheimer’s disease increased to 104 images, and the samples of normal controls increased to 108 images, where all images resized to  $255 \times 255$  pixels and normalized by rescaling the pixels to a range between zero and one.

### 3.3. Proposed Framework

CNN is a kind of feedforward artificial neural network that is popularly used for image recognition purposes. It can operate directly on raw input such as pixels, which effectively automates feature selection [75]. A general model of CNN consists of four components, namely, input layer, convolution layer, pooling layer, fully connected layer, and output layer. Figure 5 shows the basic architecture of a CNN model that performs two main tasks, which are feature extraction and classification.

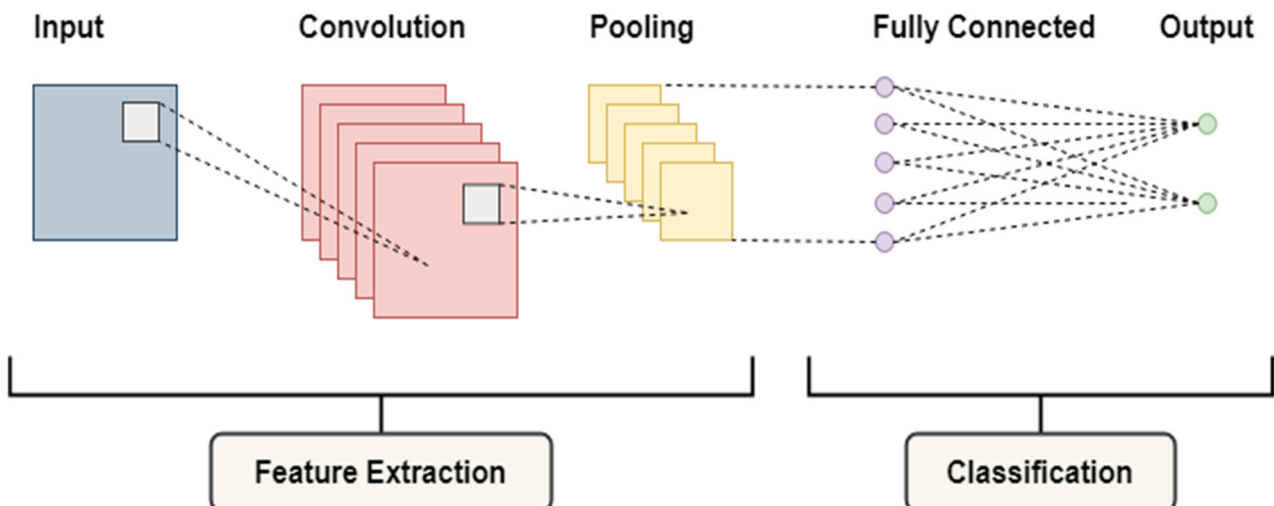


**Figure 5.** Architecture of the basic CNN approach.

The convolution operation is defined by slicing the weight vector horizontally and vertically over the input vector to generate a feature map. It takes an input image and extracts  $N$  number of features in a layer representing different features, which leads to a map of  $N$  features. After applying convolution operation, the output in the next layer for  $(i, j)$  location was calculated based on Equation (3).

$$a_{ij} = \alpha((W * X)_{ij} + b) \quad (3)$$

where  $X$  represents the input fed into the layer,  $W$  represents the weight vector that slides over input,  $b$  represents the bias, and  $\alpha$  represents the introduced non-linearity in the network.

A convolutional layer is followed by a pooling layer, which helps reduce map size, in which it introduces translation invariance. Pooling operation is performed by selecting a window, where the elements of the input lying in the window are passed through the pooling function that generates different output vectors.

Since the data set of this research is small, the classification accuracy rate would be relatively low in case the CNN are trained from the scratch by backpropagation to extract the features [76]. Hence, multiple pretrained CNN models were utilized to extract more accurate features for the classification through transfer learning. In transfer learning, the network model uses pretrained network with preset weights. ImageNet is an image database organized according to the WordNet hierarchy, in which each node of the hierarchy is depicted by hundreds and thousands of images, which are available for free to researchers for non-commercial use. In this research, two popular architectures that were trained using ImageNet are used including:

1. InceptionV3: The third version of GoogleNet, a CNN architecture released in 2015 by Google [68]. It has won the ILSVRC championship in 2015 and improving the Top-1 performance by 15% using 92 MB of parameters. InceptionV3 uses 48 layers of neural networks with 23,851,784 parameters and 159 depth size. The network has an image input size of  $299 \times 299$ , and it has learned rich feature representations for a wide range of images. Figure 6 shows the main architecture of the InceptionV3 model.
2. DenseNet201: The third version of densely connected convolutional networks (DenseNet), a CNN architecture released in 2017 CVPR and jointly invented by Cornwell University, Tsinghua University, and Facebook AI Research (FAIR) [69,77]. It is improving the Top-1 performance by 77.3% using 80 MB of parameters. DenseNet-201 uses 201 layers of neural networks with 20,242,984 parameters. The network has an image input size of  $224 \times 224$  and has learned rich feature representations for a wide range of images. Figure 7 shows the main architecture of the DenseNet201 model.

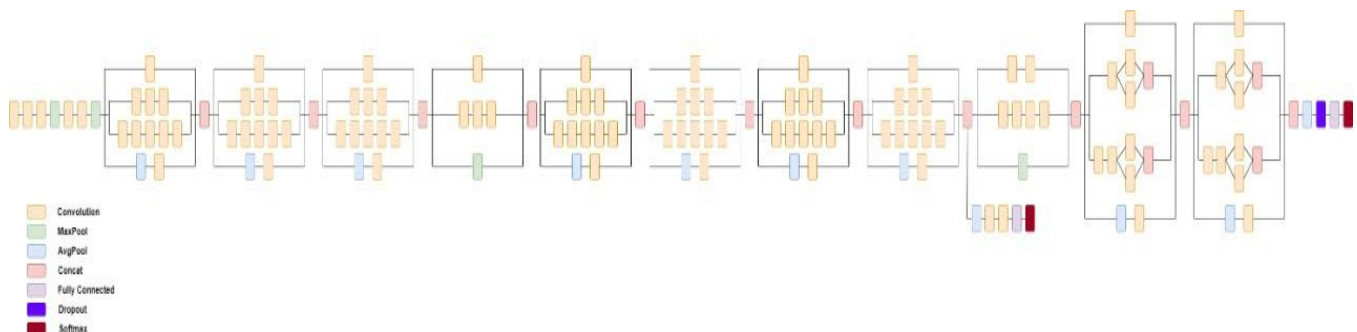
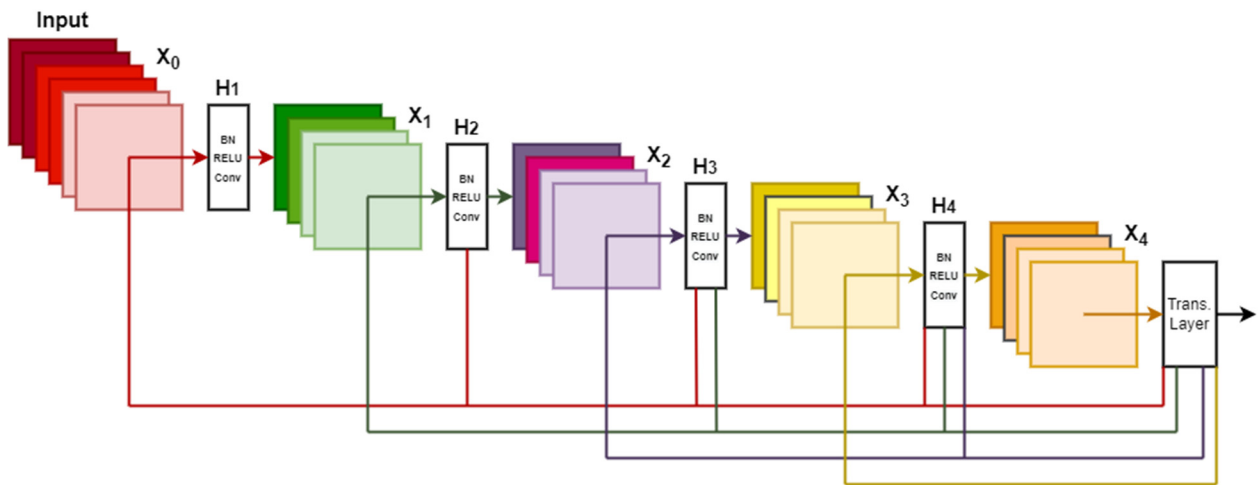


Figure 6. Architecture of InceptionV3 model.



**Figure 7.** Architecture of DenseNet201 model.

The main idea of this research is to extract the features of each image through InceptionV3 and DenseNet201 models, where the features are extracted from the last layer of each architecture, separately. Then, a combination of features is taken as follows:

$$X = (x_{11} \dots x_{1j} \dots \dots \dots x_{m1} \dots x_{mj}),$$

$(m \times j)$  dimensional matrix, where  $m$  is the total number of samples and  $j$  is the dimension of the feature.

$$Y = (y_{11} \dots y_{1k} \dots \dots \dots y_{m1} \dots y_{mk}),$$

$(m \times k)$  dimensional matrix, where  $m$  is the total number of samples and  $k$  is the dimension of the feature.

$$Z = (z_{11} \dots z_{1n} \dots \dots \dots z_{m1} \dots z_{mn}),$$

$(m \times n)$  dimensional matrix, where  $m$  is the total number of samples and  $n$  is the dimension of the feature that represents the combination of  $j$  and  $k$  features from  $X$  and  $Y$  matrices.

In case the features extracted from the last layer of the architectures, this will generate a huge number of features, in which the classifiers may fall in the problem of over-fitting. Thus, Principal Component Analysis (PCA) method utilize for feature selection through choosing the attributes that have explained variance ratio of 99% to avoid overfitting.

Subsequently, the combination of the extracted features was used to train different classical machine learning algorithms that imply binary classes: Alzheimer’s disease and normal controls. The binary classification is a problem where each record could belong to two distinct classes. Hence, three machine learning algorithms are used to train different classifiers, which are SVM, LR, LDA, and SGD [62]. Since both pretrained models generate different features from the scans, the primary idea of this research is to combine features extracted by both models and fed the selected features by PCA method into classical machine learning classifiers for more enhancement.

The K-fold cross validation method utilized to split the dataset into training and testing sets with 10-Folds, which helps to generalize the training and testing process on the whole dataset. Based on training and testing results, each model was evaluated based on the values generated by the confusion matrix [78], which is shown in Table 4.

**Table 4.** The confusion matrix.

		Predicted Values	
		Negative	Positive
Actual values	Negative	TN	FP
	Positive	FN	TP

Then, the appropriate metrics were calculated [79], which are accuracy, precision, recall, and F1-score represented by Equations (4)–(7), respectively, for further comparison between classifiers' performance.

$$ACC. = \frac{TP + TN}{TP + FP + TN + FN} \quad (4)$$

$$PREC. = \frac{TP}{TP + FP} \quad (5)$$

$$REC. = \frac{TP}{TP + FN} \quad (6)$$

$$F1 = \frac{(2 \times PREC. \times REC.)}{(PREC. + REC.)} \quad (7)$$

Accuracy is the overall accuracy of the test set. Sensitivity is a measure of how well a model can correctly identify the number of positive samples in all positive samples. Similarly, specificity is a measure of how well a model can correctly identify the number of negative samples in all negative samples. Precision refers to how many samples are predicted correctly in the positive samples. F1-score is an indicator to check the balance between precision and sensitivity. The closer the value of F1-scores is to one, the better the performance of the model.

#### 4. Experimental Results

The research experiments were carried out using a (HP) computer with a 2.21GHz CPU Intel Core (TM) i7-850H, and a memory of 32GB. The operating system is windows 10, and the software that has been used is Python (3.9).

##### 4.1. Experiments

Three experiments were conducted based on utilizing different features: the first experiment adopts features extracted using the DenseNet201 model, the second experiment adopts features extracted using the InceptionV3 model, and the third experiment adopts the combination of features extracted using both InceptionV3 and DenseNet201 models. Figure 8 shows the number of features extracted using each pre-trained model.

The number of extracted features from each pre-trained model looks huge, and that's why PCA method utilized for dimensionality reduction, in which the features were reduced into 236 and 247 for DenseNet and InceptionV3, respectively. Based on the reduced features of each pre-trained model, the classifiers were trained and tested for evaluation using 10-Fold cross validation method.

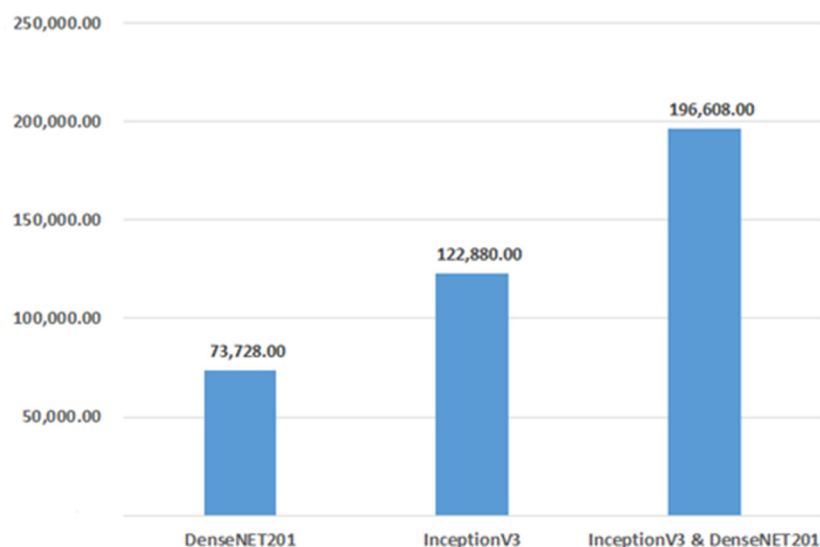


Figure 8. Number of features extracted using different pre-trained models.

4.2. Results

The performance of each classifier was evaluated by calculating the evaluation metrics based on the confusion matrix of each model. Table 5 shows the performance of classifiers based on the features generated by each model on the dataset. By comparing the classifiers’ performance that was trained on the same features, we can find that the LR classifier has achieved the best results for all feature extraction methods.

Table 5. Performance of the classifiers on different type of features.

Features Extractor	Classifier	ACC.	PREC.	REC.	F1
DenseNet201	SVM	98.57 ± 0.23	98.75 ± 0.37	98.44 ± 0.32	98.52 ± 0.24
	LR	<b>99.14 ± 0.18</b>	<b>99.98 ± 0.01</b>	<b>98.00 ± 0.42</b>	<b>98.94 ± 0.22</b>
	LDA	71.43 ± 0.59	67.91 ± 0.81	82.52 ± 1.02	74.14 ± 0.73
	SGD	94.29 ± 0.38	99.98 ± 0.01	96.89 ± 0.52	97.10 ± 0.33
InceptionV3	SVM	<b>98.29 ± 0.22</b>	<b>99.98 ± 0.01</b>	<b>96.47 ± 0.46</b>	<b>98.14 ± 0.24</b>
	LR	98.00 ± 0.22	99.98 ± 0.01	96.03 ± 0.45	97.92 ± 0.23
	LDA	70.29 ± 0.69	65.85 ± 0.71	86.46 ± 0.10	74.32 ± 0.67
	SGD	96.00 ± 0.36	99.98 ± 0.01	95.34 ± 0.33	95.02 ± 0.49
InceptionV3 + DenseNet201	SVM	98.86 ± 0.19	99.98 ± 0.01	97.74 ± 0.43	98.67 ± 0.22
	LR	<b>99.14 ± 0.18</b>	<b>99.98 ± 0.01</b>	<b>98.44 ± 0.32</b>	<b>99.19 ± 0.17</b>
	LDA	67.71 ± 0.66	64.20 ± 0.99	83.30 ± 0.97	72.01 ± 0.81
	SGD	97.71 ± 0.21	99.98 ± 0.01	95.22 ± 0.52	97.96 ± 0.33

Note: The bold number refer to the best value.

According to the results generated based on the DenseNet201 method, LR has outperformed other classifiers, where it has achieved 99.14% of accuracy, 99.98% of precision, 98.00% of recall, and predicted 1.06% of the dataset, incorrectly, with 98.94% of f1-score. As shown in Figure 9, the remaining classifiers have achieved less performance with 98.57%, 94.29%, and 71.43% accuracy levels for SVM, SGD, and LDA, respectively. A remarkable difference was shown between LR and remain classifiers based on the ability to identify Alzheimer’s disease instances.

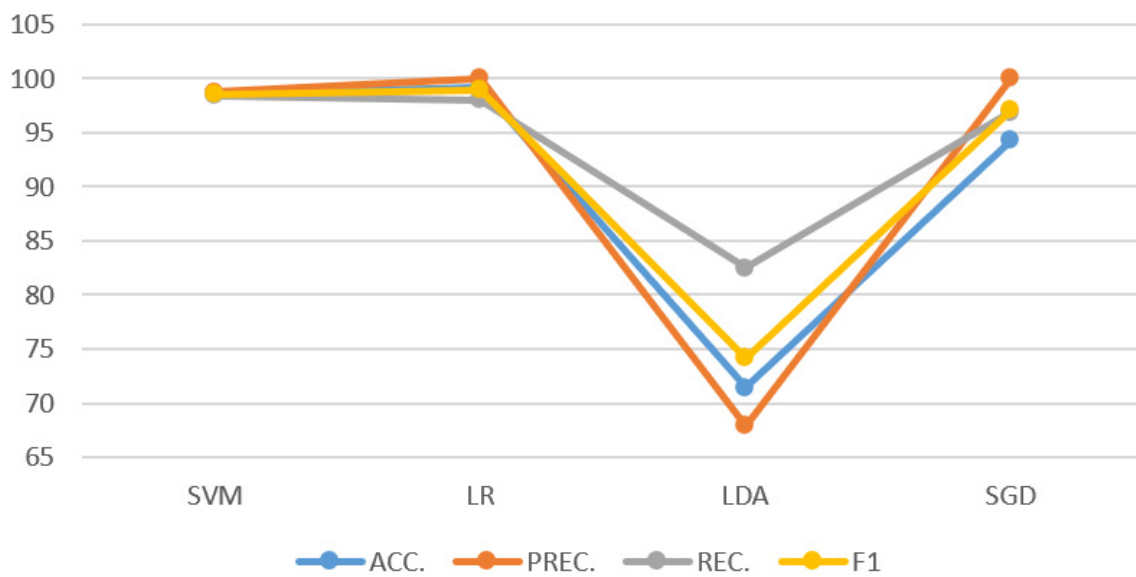


Figure 9. Performance of LR classifier on DenseNet201 features.

However, SVM with InceptionV3 features has achieved the highest results in comparison with other classifiers, where it has obtained 98.29% of accuracy, 99.98% of precision, 96.47% of recall, and predicted 1.86% of the dataset, incorrectly, with 98.14% of F1-score. The remaining classifiers had achieved less performance with 98.00%, 96.00%, and 70.29% accuracy levels for LR, SGD, and LDA, respectively. As shown in Figure 10, a remarkable difference was shown between SVM and remain classifiers based on the ability to identify Alzheimer’s disease instances. Regardless of the high score of sensitivity of the Dense201 model, the InceptionV3 model has achieved higher performance based on the remaining metrics values.

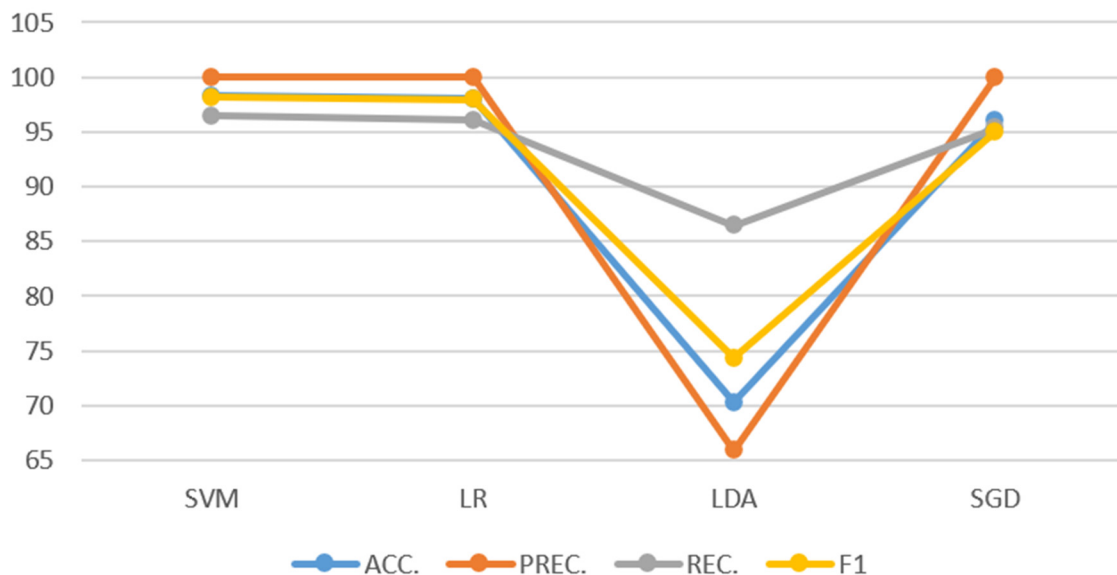
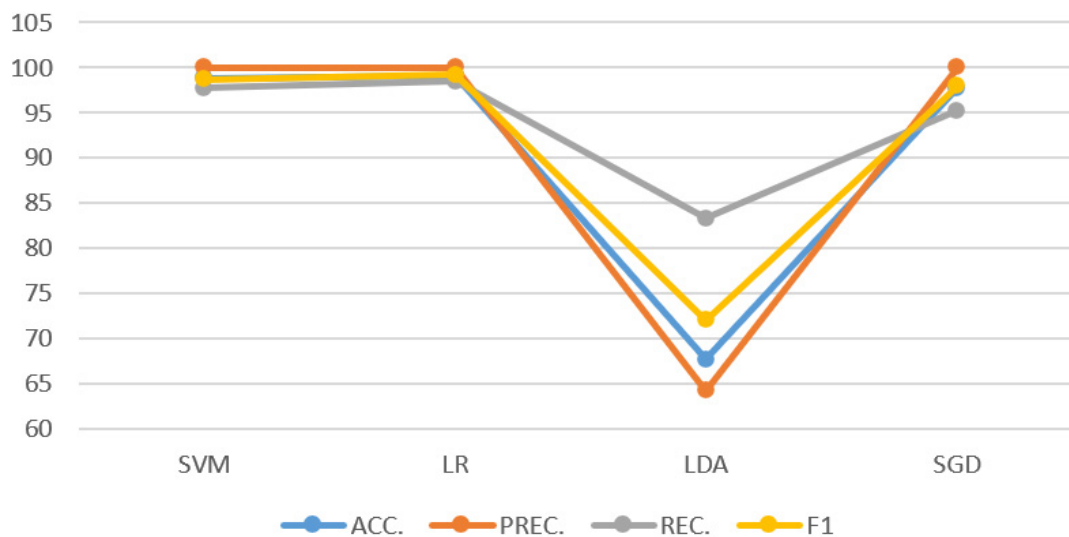


Figure 10. Performance of classifiers on InceptionV3 features.

Finally, the proposed model in this research has achieved the best performance in comparison with both previous models. According to the results in Table 5, the LR classifier has achieved the best results in comparison with other classifiers, where it has obtained 99.14% of accuracy, 99.98% of precision, 98.44% of recall, and predicted 0.81% of the dataset, incorrectly, with 99.17% of f1-score. The remaining classifiers had achieved less performance with 98.86%, 97.71%, and 67.71% accuracy levels for SVM, SGD, and LDA,

respectively. As shown in Figure 11, the same remarkable difference was shown between LR and remain classifiers based on the ability to identify Alzheimer's disease instances. Regardless of the high score of sensitivity of the Dense201 model, the proposed model of InceptionV3 and Dense201 has achieved the highest performance based on the remaining metrics values.



**Figure 11.** Performance of classifiers on features extracted from both InceptionV3 and DenseNet201.

Consequently, we can see that LR achieved higher results in comparison with the remaining classifiers remarkably. Regardless of the high score of specificity and precision of the InceptionV3 model, the proposed model could tradeoff between the whole metrics and benefit from the features of both models, in which it has achieved the highest performance.

The evaluation of classifiers showed that the features that were extracted using InceptionV3 were more powerful than features extracted using DenseNet201, as LR has performed better with an increase of 0.85% of accuracy level and 0.80% of the correct predicted form the whole instances. Regardless, we believe in our proposed model that InceptionV3 and DenseNet201 generate different features, and these features can be combined to enhance the classification task. According to the results of the third experiment, it has shown that our proposed model outperformed other models, as LR has performed better than the first experiment with an increase of 0.85% of accuracy level and 1.05% of the correct predicted form the whole instances. Moreover, it has performed better than the second experiment with an increase of 0.25% of the correct predicted form the whole instances.

#### 4.3. Comparison with Previous Works

In comparison with the previous works, this proposed methodology has achieved accurate and effective results through utilizing scans of few participants and considered as the first research that leans on cerebral blood flow biomarkers for Alzheimer's disease based on DSA scans, which can help the radiologists find the appropriate treatment plan for the eradication of Alzheimer's disease.

According to the data in Table 6, which represents a comparison between our proposed research and the previous research, our research considered as the first research that utilized cerebral blood flow biomarker from DSA scans for Alzheimer's disease detection. Moreover, it has outperformed the previous works [52–57,60,61,63–67] in terms of accuracy with a 96.7% score. To guarantee a fair comparison, the researchers in [61,65,66] have utilized 3D and 4D scans in their methodologies, while our proposed methodology utilized 2D scans of distinct modality. Additionally, the researchers in [63] utilized two databases and train their model on about thousand samples, while our proposed model has trained on few numbers of samples, and it has obtained efficient results.

**Table 6.** Comparison between previous works and the proposed method.

Study	Modality	Feature Extraction Method	Classifier	AD	NC	ACC.
Lebedev et al. [52]	Structural MRI	Surface-based registration	Random Forest	185	225	90.30
Zhang and Wang [53]	3D-MRI	Displacement Field	Twin SVM	28	98	92.70
Beheshti et al. [54]	Structural MRI	Voxel-based feature extraction	SVM	130	130	92.40
Zhang et al. [55]	Structural MRI	Bag-of-words	SVM	154	207	88.30
Zeng et al. [56]	MRI	Anatomical Labeling	SDPSO-SVM-PCA	92	82	71.20
Koh et al. [57]	MRI	BE Mode Decomposition	SVM-Poly-1	55	110	93.90
Liu et al. [60]	3D-FDG-PET	2D-CNN and BGRU	Softmax	93	100	91.20
Ge et al. [61]	3D-MRI	3D-multiscale-CNN	XGBoost	198	139	98.20
Basaia et al. [6]	MRI	CNN	LR	542	457	98.00
Pan et al. [64]	MRI	2D-CNN	Ensemble	137	162	84.00
Feng et al. [65]	3D-MRI	3D-CNN	SVM	153	159	99.10
Li et al. [66]	4D-MRI	3D-CNN and LSTM	Softmax	116	174	97.30
Liu et al. [67]	MRI	GoogleNet	Softmax	30	332	93.00
Proposed Research	DSA	InceptionV3 + DenseNet201	LR	13	27	99.14

Finally, based on the comparison with the previous works, this research achieved accurate and effective results through utilizing scans of a few participants and considered as the first research that leans on cerebral blood flow biomarker for Alzheimer's disease based on DSA scans, which can help the radiologists find the appropriate treatment plan for eradication of Alzheimer's disease. Finally, the proposed approach of this research considered state-of-the-art for the early diagnosis of Alzheimer's disease using cerebral blood flow biomarkers from DSA scans.

## 5. Conclusions and Future Work

Alzheimer's disease is hard to be cured, and it afflicts the patient for the rest of their life. Lately, it has been found that the number of people suffering from Alzheimer's disease is increasing. The early diagnosis of Alzheimer's disease is important to avoid the deterioration of the patient situation. In this paper, a novel approach was devised based on a DSA scan that showed the features of a new biomarker cerebral blood flow. The used dataset was acquired from the database of K.A.U.H hospital and contains digitally subtracted angiograms of participants who were diagnosed with Alzheimer's disease, besides samples of normal controls. Since each scan included multiple frames for the left and right ICA's, pre-processing steps were applied to make the dataset prepared for the next stages of feature extraction and classification. The multiple frames of scans transformed from real space into DCT space and averaged to remove noises. Then, the averaged image was transformed back to the real space, and both sides were filtered with Meijering and concatenated in a single image. The proposed model extracted the features using different pre-trained models: InceptionV3 and DenseNet201. Then, the PCA method was utilized to select the features with 0.99, explained variance ratio, where the combination of selected features from both pre-trained models were fed into machine learning classifiers. Overall, the obtained experimental results were at least as good as other state-of-the-art approaches in the literature and more efficient according to the recent medical standards with a 99.14% level of accuracy, considering the difference in dataset samples and the used cerebral blood flow biomarker. Considering the limited quantity of the available DSA scans for patients who have been diagnosed with Alzheimer's disease, we assume that the new biomarker of cerebral blood flow can be further extracted with more samples that may have a smaller variance.

As for future work, we aim to collect more samples, in which we can design new CNN architecture that generates more accurate results besides conducting segmentation experiments to assist the treatment plan of radiologists.

**Author Contributions:** Conceptualization, methodology, and writing—review and editing, M.G.; Conceptualization, supervision, methodology, visualization, software, validation, formal analysis, investigation, resources, writing—review and editing, M.A.; Supervision, and writing—review and editing, M.Z.A.; Supervision, and writing—review and editing, A.A.-B.; Conceptualization, methodology, and writing—review and editing, M.E.-H.; Conceptualization, methodology, and writing—review and editing, L.A.; Conceptualization, methodology, and writing—review and editing, M.A.; Conceptualization, methodology, and writing—review and editing, A.A.; Conceptualization, methodology, and writing—review and editing, A.H.G. All authors have read and agreed to the published version of the manuscript.

**Funding:** Authors gratefully acknowledge the support of the Deanship of Research at the Jordan University of Science and Technology for supporting this work via Grant 20210223. This study was financially supported via a funding grant by Deanship of Scientific Research, Taif University Researchers Supporting Project number (TURSP-2020/300), Taif University, Taif, Saudi Arabia.

**Institutional Review Board Statement:** Institutional Review Board Committee of Jordan University of Science and Technology approved this study, (Ref number: 2021-162).

**Informed Consent Statement:** Informed consent was obtained from all subjects involved in the study.

**Data Availability Statement:** The data will be available upon request.

**Acknowledgments:** The authors would like to thank King Abdullah University Hospital for providing data for this paper.

**Conflicts of Interest:** The authors declare no conflict of interest.

## References

1. Leone, M.; Cecchini, A.P.; Mea, E.; Tullo, V.; Curone, M.; Bussone, G. Neuroimaging and pain: A window on the autonomic nervous system. *Neurol. Sci.* **2006**, *27*, s134–s137. [\[CrossRef\]](#)
2. Camprodon, J.A.; Stern, T.A. Selecting neuroimaging techniques: A review for the clinician. *Australas. Psychiatry* **2013**. [\[CrossRef\]](#)
3. Zhang, Z.; Sejdić, E. Radiological images and machine learning: Trends, perspectives, and prospects. *Comput. Biol. Med.* **2019**, *108*, 354–370. [\[CrossRef\]](#) [\[PubMed\]](#)
4. Taboada-Crispi, A.; Sahli, H.; Hernandez-Pacheco, D.; Falcon-Ruiz, A. Anomaly detection in medical image analysis. In *Handbook of Research on Advanced Techniques in Diagnostic Imaging and Biomedical Applications*; IGI Global: Hershey, PA, USA, 2009; pp. 426–446.
5. Klöppel, S.; Abdulkadir, A.; Jack, C.R., Jr.; Koutsouleris, N.; Mourão-Miranda, J.; Vemuri, P. Diagnostic neuroimaging across diseases. *Neuroimage* **2012**, *61*, 457–463. [\[CrossRef\]](#)
6. Bruffaerts, R. Machine learning in neurology: What neurologists can learn from machines and vice versa. *J. Neurol.* **2018**, *265*, 2745–2748. [\[CrossRef\]](#) [\[PubMed\]](#)
7. Li, Q.; Cai, W.; Wang, X.; Zhou, Y.; Feng, D.D.; Chen, M. Medical image classification with convolutional neural network. In Proceedings of the 2014 13th International Conference on Control Automation Robotics & Vision IEEE (ICARCV), Singapore, 10–12 December 2014; pp. 844–848.
8. Cortes-Canteli, M.; Iadecola, C. Alzheimer’s disease and vascular aging: JACC focus seminar. *J. Am. Coll. Cardiol.* **2020**, *75*, 942–951. [\[CrossRef\]](#) [\[PubMed\]](#)
9. Korte, N.; Nortley, R.; Attwell, D. Cerebral blood flow decrease as an early pathological mechanism in Alzheimer’s disease. *Acta Neuropathol.* **2020**, *40*, 793–810. [\[CrossRef\]](#) [\[PubMed\]](#)
10. Dai, W.; Lopez, O.L.; Carmichael, O.T.; Becker, J.T.; Kuller, L.H.; Gach, H.M. Mild Cognitive Impairment and Alzheimer Disease: Patterns of Altered Cerebral Blood Flow at MR Imaging. *Radiology* **2009**, *250*, 856–866. [\[CrossRef\]](#) [\[PubMed\]](#)
11. Bennett, R.E.; Robbins, A.B.; Hu, M.; Cao, X.; Betensky, R.A.; Clark, T.; Das, S.; Hyman, B.T. Tau induces blood vessel abnormalities and angiogenesis-related gene expression in P301L transgenic mice and human Alzheimer’s disease. *Proc. Natl. Acad. Sci. USA* **2018**, *115*, E1289–E1298. [\[CrossRef\]](#) [\[PubMed\]](#)
12. Decker, Y.; Müller, A.; Németh, E.; Schulz-Schaeffer, W.J.; Fatar, M.; Menger, M.D.; Liu, Y.; Fassbender, K. Analysis of the vasculature by immunohistochemistry in paraffin-embedded brains. *Brain Struct. and Funct.* **2018**, *223*, 1001–1015. [\[CrossRef\]](#)
13. De Strooper, B.; Karran, E. The cellular phase of Alzheimer’s disease. *Cell* **2016**, *164*, 603–615. [\[CrossRef\]](#) [\[PubMed\]](#)
14. Alloui, H.; Sadgal, M.; Elfazziki, A. Utilization of a convolutional method for Alzheimer disease diagnosis. *Mach. Vis. Appl.* **2020**, *31*, 25. [\[CrossRef\]](#)
15. National Institute of Neurological, Communicative Disorders, Stroke. Office of Scientific and Health Reports. In *The Dementias: Hope through research (No. 81)*; US Department of Health and Human Services, Public Health Service, National Institutes of Health: Bethesda, MD, USA, 1981.
16. Duff, C. Dementia: Assessment, Management and Support for People Living with Dementia and their Carers. Available online: <https://eprints.lincoln.ac.uk/id/eprint/38978/> (accessed on 29 November 2021).

17. Ambrose, C.T. Alzheimer's Disease: The Great Morbidity of the 21st Century. *Am. Sci.* **2013**, *100*, 194. [[CrossRef](#)]
18. Livingston, G.; Huntley, J.; Sommerlad, A.; Ames, D.; Ballard, C.; Banerjee, S.; Brayne, C.; Burns, A.; Cohen-Mansfield, J.; Cooper, C.; et al. Dementia prevention, intervention, and care: 2020 report of the Lancet Commission. *Lancet* **2020**, *396*, 413–446. [[CrossRef](#)]
19. Nichols, E.; Szeoke, C.E.; Vollset, S.E.; Abbasi, N.; Abd-Allah, F.; Abdela, J.; Aichour, M.T.E.; Akinyemi, R.O.; Alahdab, F.; Asgedom, S.W.; et al. Global, regional, and national burden of Alzheimer's disease and other dementias, 1990–2016: A systematic analysis for the Global Burden of Disease Study 2016. *Lancet Neurol.* **2019**, *18*, 88–106. [[CrossRef](#)]
20. Lancet, T. The Three Stages of Alzheimer's Disease. Available online: [https://www.thelancet.com/journals/lancet/article/PIIS0140-6736\(20\)32205-4/fulltext](https://www.thelancet.com/journals/lancet/article/PIIS0140-6736(20)32205-4/fulltext) (accessed on 29 November 2021).
21. Márquez, F.; Yassa, M.A. Neuroimaging Biomarkers for Alzheimer's Disease. *Mol. Neurodegener.* **2019**, *14*, 21. [[CrossRef](#)] [[PubMed](#)]
22. Alzheimer's Association. 2018 Alzheimer's disease facts and figures. *Alzheimer's Dement.* **2018**, *14*, 367–429. [[CrossRef](#)]
23. Veitch, D.P.; Weiner, M.W.; Aisen, P.S.; Beckett, L.A.; Cairns, N.J.; Green, R.C.; Harvey, D.; Jack, C.R., Jr.; Jagust, W.; Morris, J.C.; et al. Understanding disease progression and improving Alzheimer's disease clinical trials: Recent highlights from the Alzheimer's Disease Neuroimaging Initiative. *Alzheimer's Dement.* **2019**, *15*, 106–152. [[CrossRef](#)]
24. Kwong, R.Y.; Yucel, E.K. Computed Tomography Scan and Magnetic Resonance Imaging. *Circulation* **2003**, *108*, e104–e106. [[CrossRef](#)]
25. Zhang, Y.; Londos, E.; Minthon, L.; Wattmo, C.; Liu, H.; Aspelin, P.; Wahlund, L.O. Usefulness of computed tomography linear measurements in diagnosing Alzheimer's disease. *Acta Radiol.* **2008**, *49*, 91–97. [[CrossRef](#)] [[PubMed](#)]
26. Van Beek, E.J.; Kuhl, C.; Anzai, Y.; Desmond, P.; Ehman, R.L.; Gong, Q.; Gold, G.; Gulani, V.; Hall-Craggs, M.; Leiner, T.; et al. Value of MRI in medicine: More than just another test? *J. Magn. Reson. Imaging* **2018**, *49*, e14–e25. [[CrossRef](#)] [[PubMed](#)]
27. Silverman, D.H.; Small, G.W.; Chang, C.Y.; Lu, C.S.; de Aburto, M.A.K.; Chen, W.; Czernin, J.; Rapoport, S.I.; Pietrini, P.; Alexander, G.E.; et al. Positron emission tomography in evaluation of dementia: Regional brain metabolism and long-term outcome. *Jama* **2001**, *286*, 2120–2127. [[CrossRef](#)]
28. Duggall, N.J.; Bruggink, S.; Ebmeier, K.P. Systematic Review of the Diagnostic Accuracy of 99mTc-HMPAO-SPECT in Dementia. Available online: <https://www.ncbi.nlm.nih.gov/books/NBK70560/> (accessed on 29 November 2021).
29. Dubois, B.; Feldman, H.H.; Jacova, C.; Hampel, H.; Molinuevo, J.L.; Blennow, K.; DeKosky, S.T.; Gauthier, S.; Selkoe, D.; Bateman, R.; et al. Advancing research diagnostic criteria for Alzheimer's disease: The IWG-2 criteria. *Lancet Neurol.* **2014**, *13*, 614–629. [[CrossRef](#)]
30. Frisoni, G.B.; Fox, N.C.; Clifford, R.J., Jr.; Scheltens, P.; Thompson, P. The clinical use of structural MRI in Alzheimer disease. *Nat. Rev. Neurol.* **2010**, *6*, 67–77. [[CrossRef](#)]
31. Schwab, K.E.; Gailloud, P.; Wyse, G.; Tamargo, R.J. Limitations of magnetic resonance imaging and magnetic resonance angiography in the diagnosis of intracranial aneurysms. *Neurosurgery* **2008**, *63*, 29–35. [[CrossRef](#)]
32. Ungvari, Z.; Tarantini, S.; Donato, A.J.; Galvan, V.; Csiszar, A. Mechanisms of Vascular Aging. *Circ. Res.* **2018**, *123*, 849–867. [[CrossRef](#)] [[PubMed](#)]
33. Roher, A.E.; Esh, C.; Rahman, A.; Kokjohn, T.A.; Beach, T.G. Atherosclerosis of Cerebral Arteries in Alzheimer Disease. *Stroke* **2004**, *35*, 2623–2627. [[CrossRef](#)] [[PubMed](#)]
34. Bullitt, E.; Zeng, D.; Mortamet, B.; Ghosh, A.; Aylward, S.R.; Lin, W.; Marks, B.L.; Smith, J.K. The effects of healthy aging on intracerebral blood vessels visualized by magnetic resonance angiography. *Neurobiol. Aging* **2010**, *31*, 290–300. [[CrossRef](#)]
35. Abualigah, L.; Diabat, A.; Sumari, P.; Gandomi, A.H. A novel evolutionary arithmetic optimization algorithm for multilevel thresholding segmentation of covid-19 ct images. *Processes* **2021**, *9*, 1155. [[CrossRef](#)]
36. Salmon, E.; Ir, C.B.; Hustinx, R. Pitfalls and Limitations of PET/CT in Brain Imaging. *Semin. Nucl. Med.* **2015**, *45*, 541–551. [[CrossRef](#)]
37. Alzheimer's Disease Neuroimaging Initiative (ADNI). Available online: <http://adni.loni.usc.edu/> (accessed on 25 July 2021).
38. Harvard Medical School Data. Available online: <http://www.med.harvard.edu/AANLIB/> (accessed on 16 March 2021).
39. Marcus, D.S.; Wang, T.H.; Parker, J.; Csernansky, J.G.; Morris, J.C.; Buckner, R.L. Open Access Series of Imaging Studies (OASIS): Cross-sectional MRI Data in Young, Middle Aged, Nondemented, and Demented Older Adults. *J. Cogn. Neurosci.* **2007**, *19*, 1498–1507. [[CrossRef](#)]
40. Thambisetty, M.; Beasonheld, L.L.; An, Y.; Kraut, M.A.; Resnick, S.M. APOE  $\epsilon$ 4 Genotype and Longitudinal Changes in Cerebral Blood Flow in Normal Aging. *Arch. Neurol.* **2010**, *67*, 93–98. [[CrossRef](#)]
41. Stergaard, L.; Aamand, R.; Gutiérrez-Jiménez, E.; Ho, Y.C.L.; Blicher, J.U.; Madsen, S.M.; Nagenthiraja, K.; Dalby, R.B.; Drasbek, K.R.; Møller, A.; et al. The capillary dysfunction hypothesis of Alzheimer's disease. *Neurobiol. Aging* **2013**, *34*, 1018–1031. [[CrossRef](#)]
42. Harvard Medical School. Carotid Artery Disease. 2021. Available online: <https://www.health.harvard.edu/heartdisease/carotid-artery-disease-overview> (accessed on 25 July 2021).
43. Fazlollahi, A.; Calamante, F.; Liang, X.; Bourgeat, P.; Raniga, P.; Dore, V.; Fripp, J.; Ames, D.; Masters, C.L.; Rowe, C.C.; et al. Increased cerebral blood flow with increased amyloid burden in the preclinical phase of alzheimer's disease. *J. Magn. Reson. Imaging* **2020**, *51*, 505–513. [[CrossRef](#)]

44. Guo, Y.; Li, X.; Zhang, M.; Chen, N.; Wu, S.; Lei, J.; Wang, Z.; Wang, R.; Wang, J.; Liu, H. Age and brain region associated alterations of cerebral blood flow in early Alzheimer's disease assessed in A $\beta$ PPSWE/PS1 $\Delta$ E9 transgenic mice using arterial spin labeling. *Mol. Med. Rep.* **2019**, *19*, 3045–3052. [[CrossRef](#)]
45. Lin, S.; Jia, H.; Abualigah, L.; Altalhi, M. Enhanced Slime Mould Algorithm for Multilevel Thresholding Image Segmentation Using Entropy Measures. *Entropy* **2021**, *23*, 1700. [[CrossRef](#)]
46. Alomari, O.A.; Khader, A.T.; Al-Betar, M.A.; Abualigah, L.M. Gene selection for cancer classification by combining minimum redundancy maximum relevancy and bat-inspired algorithm. *Int. J. Data Min. Bioinform.* **2017**, *19*, 32–51. [[CrossRef](#)]
47. Shehab, M.; Daoud, M.S.; AlMimi, H.M.; Abualigah, L.M.; Khader, A.T. Hybridising cuckoo search algorithm for extracting the ODF maxima in spherical harmonic representation. *Int. J. Bio-Inspired Comput.* **2019**, *14*, 190–199. [[CrossRef](#)]
48. Sawiris, N.; Venizelos, A.; Ouyang, B.; Lopes, D.; Chen, M. Current Utility of Diagnostic Catheter Cerebral Angiography. *J. Stroke Cerebrovasc. Dis.* **2014**, *23*, e145–e150. [[CrossRef](#)]
49. Alakbarzade, V.; Pereira, A. Cerebral catheter angiography and its complications. *Pr. Neurol.* **2018**, *18*, 393–398. [[CrossRef](#)]
50. Rathore, S.; Habes, M.; Iftikhar, M.A.; Shacklett, A.; Davatzikos, C. A review on neuroimaging-based classification studies and associated feature extraction methods for Alzheimer's disease and its prodromal stages. *NeuroImage* **2017**, *155*, 530–548. [[CrossRef](#)]
51. Samper-González, J.; Burgos, N.; Bottani, S.; Fontanella, S.; Lu, P.; Marcoux, A.; Routier, A.; Guillon, J.; Bacci, M.; Wen, J.; et al. Reproducible evaluation of classification methods in Alzheimer's disease: Framework and application to MRI and PET data. *NeuroImage* **2018**, *183*, 504–521. [[CrossRef](#)]
52. Lebedev, A.V.; Westman, E.; Van Westen, G.J.P.; Kramberger, M.G.; Lundervold, A.; Aarsland, D.; Soininen, H.; Kłoszewska, I.; Mecocci, P.; Tsolaki, M.; et al. Random Forest ensembles for detection and prediction of Alzheimer's disease with a good between-cohort robustness. *NeuroImage Clin.* **2014**, *6*, 115–125. [[CrossRef](#)] [[PubMed](#)]
53. Zhang, Y.; Wang, S. Detection of Alzheimer's disease by displacement field and machine learning. *PeerJ* **2015**, *3*, e1251. [[CrossRef](#)]
54. Beheshti, I.; Demirel, H.; Farokhian, F.; Yang, C.; Matsuda, H.; Alzheimer's Disease Neuroimaging Initiative. Structural MRI-based detection of Alzheimer's disease using feature ranking and classification error. *Comput. Methods Programs Biomed.* **2016**, *137*, 177–193. [[CrossRef](#)]
55. Zhang, J.; Liu, M.; An, L.; Gao, Y.; Shen, D. Alzheimer's disease diagnosis using landmark-based features from longitudinal structural MR images. *IEEE J. Biomed. Health Inform.* **2017**, *21*, 1607–1616. [[CrossRef](#)]
56. Zeng, N.; Qiu, H.; Wang, Z.; Liu, W.; Zhang, H.; Li, Y. A new switching-delayed-PSO-based optimized SVM algorithm for diagnosis of Alzheimer's disease. *Neurocomputing* **2018**, *320*, 195–202. [[CrossRef](#)]
57. Koh, J.E.W.; Jahmunah, V.; Pham, T.H.; Oh, S.L.; Ciaccio, E.J.; Acharya, U.R.; Yeong, C.H.; Fabell, M.K.M.; Rahmat, K.; Vijayanathan, A.; et al. Automated detection of Alzheimer's disease using bi-directional empirical model decomposition. *Pattern Recognit. Lett.* **2020**, *135*, 106–113. [[CrossRef](#)]
58. Plis, S.M.; Hjelm, D.R.; Salakhutdinov, R.; Allen, E.A.; Bockholt, H.J.; Long, J.D.; Johnson, H.J.; Paulsen, J.S.; Turner, J.A.; Calhoun, V.D. Deep learning for neuroimaging: A validation study. *Front. Neurosci.* **2014**, *8*, 229. [[CrossRef](#)]
59. LeCun, Y.; Bengio, Y.; Hinton, G. Deep learning. *Nature* **2015**, *521*, 436–444. [[CrossRef](#)]
60. Liu, M.; Cheng, D.; Yan, W.; Alzheimer's Disease Neuroimaging Initiative. Classification of Alzheimer's Disease by Combination of Convolutional and Recurrent Neural Networks Using FDG-PET Images. *Front. Aging Neurosci.* **2018**, *12*, 35. [[CrossRef](#)] [[PubMed](#)]
61. Ge, C.; Qu, Q.; Gu, I.Y.-H.; Jakola, A. Multi-stream multi-scale deep convolutional networks for Alzheimer's disease detection using MR images. *Neurocomputing* **2019**, *350*, 60–69. [[CrossRef](#)]
62. Bonaccorso, G. *Machine Learning Algorithms*; Packt Publishing Ltd.: Birmingham, UK, 2017.
63. Basaia, S.; Agosta, F.; Wagner, L.; Canu, E.; Magnani, G.; Santangelo, R.; Filippi, M.; Alzheimer's Disease Neuroimaging Initiative. Automated classification of Alzheimer's disease and mild cognitive impairment using a single MRI and deep neural networks. *NeuroImage: Clin.* **2019**, *21*, 101645. [[CrossRef](#)] [[PubMed](#)]
64. Pan, D.; Zeng, A.; Jia, L.; Huang, Y.; Frizzell, T.; Song, X. Early Detection of Alzheimer's Disease Using Magnetic Resonance Imaging: A Novel Approach Combining Convolutional Neural Networks and Ensemble Learning. *Front. Neurosci.* **2020**, *14*, 259. [[CrossRef](#)] [[PubMed](#)]
65. Feng, W.; Van Halm-Lutterrodt, N.; Tang, H.; Mecum, A.; Mesregah, M.; Ma, Y.; Li, H.; Zhang, F.; Wu, Z.; Yao, E.; et al. Automated MRI-Based Deep Learning Model for Detection of Alzheimer's Disease Process. *Int. J. Neural Syst.* **2020**, *30*, 2050032. [[CrossRef](#)]
66. Li, W.; Lin, X.; Chen, X. Detecting Alzheimer's disease Based on 4D fMRI: An exploration under deep learning framework. *Neurocomputing* **2020**, *388*, 280–287. [[CrossRef](#)]
67. Liu, J.; Li, M.; Luo, Y.; Yang, S.; Li, W.; Bi, Y. Alzheimer's disease detection using depthwise separable convolutional neural networks. *Comput. Methods Programs Biomed.* **2021**, *203*, 106032. [[CrossRef](#)]
68. Chollet, F. Xception: Deep learning with depthwise separable convolutions. In Proceedings of the IEEE Conference on Computer Vision and Pattern Recognition, Honolulu, HI, USA, 21–26 July 2017; pp. 1251–1258.
69. Train Your Own Image Classifier with Inception in TensorFlow, Google AI Blog, 09-Mar-2016. Available online: <https://ai.googleblog.com/2016/03/train-your-ownimage-classifier-with.html>. (accessed on 25 July 2021).
70. Jeans, W.D. The development and use of digital subtraction angiography. *Br. J. Radiol.* **1990**, *63*, 161–168. [[CrossRef](#)] [[PubMed](#)]

71. Chilcote, W.A.; Modic, M.T.; Pavlicek, W.A.; Little, J.R.; Furlan, A.J.; Duchesneau, P.M.; Weinstein, M.A. Digital subtraction angiography of the carotid arteries: A comparative study in 100 patients. *Radiology* **1981**, *139*, 287–295. [[CrossRef](#)]
72. Yu, G.; Sapiro, G. DCT Image Denoising: A Simple and Effective Image Denoising Algorithm. *Image Process. Line* **2011**, *1*, 292–296. [[CrossRef](#)]
73. Wang, A.; Yan, X.; Wei, Z. ImagePy: An open-source, Python-based and platform-independent software package for bioimage analysis. *Bioinformatics* **2018**, *34*, 3238–3240. [[CrossRef](#)]
74. Mikołajczyk, A.; Grochowski, M. Data augmentation for improving deep learning in image classification problem. In Proceedings of the International Interdisciplinary PhD Workshop (IIPhDW), Swinoujście, Poland, 9–12 May 2018; pp. 117–122. [[CrossRef](#)]
75. Indolia, S.; Goswami, A.; Mishra, S.; Asopa, P. Conceptual Understanding of Convolutional Neural Network- A Deep Learning Approach. *Procedia Comput. Sci.* **2018**, *132*, 679–688. [[CrossRef](#)]
76. Zhang, G.; Kato, J.; Wang, Y.; Mase, K. How to initialize the CNN for small datasets: Extracting discriminative filters from pre-trained model. In Proceedings of the 2015 3rd IAPR Asian Conference on Pattern Recognition, IEEE (ACPR), Kuala Lumpur, Malaysia, 3–6 November 2015; pp. 479–483.
77. Huang, G.; Liu, Z.; Van Der Maaten, L.; Weinberger, K.Q. Densely connected convolutional networks. In Proceedings of the IEEE Conference on Computer Vision and Pattern Recognition, Honolulu, HI, USA, 21–26 July 2017; pp. 4700–4708.
78. Susmaga, R. Confusion matrix visualization. In *Intelligent Information Processing and Web Mining*; Springer: Berlin/Heidelberg, Germany, 2004; pp. 107–116.
79. Fürnkranz, J.; Flach, P.A. An analysis of rule evaluation metrics. In Proceedings of the 20th International Conference on Machine Learning (ICML-03), Washington, DC, USA, 21–24 August 2003; pp. 202–209.